Appl. Phys. B 56, 287–293 (1993)

Applied Physics B Photophysics and Laser Chemistry

Determination of Temperature by Stimulated Raman Scattering of Molecular Nitrogen, Oxygen, and Carbon Dioxide

G. Millot, B. Lavorel, G. Fanjoux, C. Wenger

Laboratoire de Spectronomie Moléculaire et Instrumentation Laser, Université de Bourgogne, U.R.A. CNRS, 6, Bd. Gabriel, F-21000 Dijon, France (Tel.: 33-80/39 59 81, Fax: 33-80/39 59 71)

Received 11 November 1992/Accepted 9 February 1993

Abstract. We have determined the temperature from SRS spectra of N_2–N_2, N_2–CO_2, O_2–O_2, and CO_2–CO_2 recorded in wide pressure and temperature ranges. The fitting procedure takes simultaneously into account the Dicke effect and motional narrowing. We have quantified the accuracy of the MEG and ECS-P models for rotational relaxation. The temperature extracted from each model is compared with thermocouple measurements. The influence of vibrational broadening and shifting is discussed in detail.

PACS: 33.70, 42.65.Dr

Modern optical techniques like coherent anti-Stokes Raman spectroscopy (CARS) or stimulated Raman spectroscopy (SRS) have been proven to be effective for temperature measurement in real combustion environments [1]. Whereas CARS has demonstrated its usefulness in many applications, SRS has been especially used for fundamental studies [2]. These fundamental studies are devoted to the determination of line broadening and line shifting coefficients over a wide temperature range and to the study of interference effects for overlapping lines. Self collisions and collisions with minor species define the Q-branch profile for the probe molecule. The main collisional systems investigated up to now are N_2–N_2 [3–13], N_2–CO_2 [14], N_2–H_2O [15], N_2–CO_2–H_2O [16], O_2–O_2, O_2–N_2 [17, 18], CO_2–CO_2 [19, 20], and CO–CO [21, 22]. Among these collisional systems, we have been particularly interested in N_2–N_2, N_2–CO_2, O_2–O_2, and CO_2–CO_2. The Q-branch Raman spectra have been recorded with the high-resolution stimulated Raman spectrometer developed at Dijon a few years ago [3, 4, 6]. The main characteristics of this laser spectrometer are, first, its high spectral resolution ($2.3 \times 10^{-3}\,cm^{-1}$), and second, its accurate absolute frequency calibration (better than $10^{-3}\,cm^{-1}$) [23]. Another characteristic is the absence of the nonresonant part of the Raman signal, since the stimulated Raman process only depends on the imaginary part of the susceptibility. We have taken advantage of these properties for developing and testing different models describing rotational relaxation rates, by comparison between calculated spectra and SRS experimental data over a wide density range. Among these models, we have focused our attention on the MEG law [7] used in practical applications and on the ECS-P law [9] which has a more physical background. The nonlinear susceptibility gives a spectral shape which depends on pressure and temperature. The synthetic shape depends on modeling of the rotational relaxation rates and consequently measurements of medium properties will also depend on the model used for these relaxation rates.

In our previous studies [9, 11, 14, 17–20], we have compared the MEG and ECS-P models and we have given prominence to their different behavior for modeling of line broadening coefficient and collisional line narrowing in the Q-branch. The main goal of this report is to explicitly test the accuracy of these models for the temperature determination. So, we have developed a computer routine which allows us to fit the temperature in wide pressure and temperature ranges, which works for a mixture of several gases and which takes simultaneously into account the Dicke effect and motional narrowing. The temperature is fit to SRS Q-branches recorded in a temperature-controlled cell equipped with a thermocouple. A large part of the data comes from previous studies, except for pure nitrogen, for which a spectrum at 730 K has been especially recorded for this work, and also except for spectra of N_2–N_2 at 140 K and CO_2–CO_2 at temperatures above 500 K (unpublished results). We have not tried to modify the models to obtain the exact temperature, our aim being to quantify the precision of each simple model for temperature fit from a more physical point of view. Many studies have been reported up to now in CARS thermometry ([24–28], and references therein), showing that several precautions should be taken in order to avoid systematic errors in the determination of the temperature. Among the parameters which may induce systematic errors let us note the nonresonant third-order susceptibility $\chi^{(3)}_{(NR)}$, the absolute frequency calibration, the spectral dispersion of the detection system, cross coherence effects between elementary CARS polarizations when a multimode pump laser source is used, nonlinearities in the response of intensified diode array detectors, effects of finite pump-laser bandwidth,

and instrumental resolution. Most of these parameters have been found to lead to significant temperature errors if not correctly included in the temperature fit. Taking $\chi^{(3)}_{\mathrm{NR}}$ as a fitting parameter may lead to good agreement between calculated and experimental spectra but may yield an incorrect temperature. All these difficulties are avoided with our SRS spectrometer with a scanning technique and consequently the determination of the temperature essentially results from the relaxation matrix modeling. For all collisional systems considere here, a few spectra have been recorded at very low pressure (about 1 Torr) for which we have not observed the effect of Stark broadening. So we estimate that fitting temperature to observed SRS spectra and comparison with thermocouple reading is a critical test of the rate laws.

1 High Temperature Furnace

The pump and probe lasers were focused using a 380 mm focal-length lens to a waist diameter of about 100 μm inside a windowed cell introduced in an electric oven. For spectra recorded at pressures below 2 bar, the Raman cell was a cylindrical quartz cell with optical Brewster windows. At pressures greater than 2 bar, a stainless steel cell equipped with sapphire windows was used. The furnace is capable of operating up to 1350 K. A crossed-beam configuration was used to avoid possible spurious signals arising from air components. The interaction length was estimated to be approximately 10 mm and is very small compared to the 400 mm length of the oven. The focal region was located at the longitudinal center of the electric oven. The longitudinal temperature gradient was negligible in the interaction volume. Temperature control and stabilization in the furnace was provided by a K-type thermocouple connected with a microprocessor to control the heating current. Special attention was given to the arrangement of the thermocouple and the interaction zone of the lasers, so that the measurement point was less than 10 mm away from the focal region. Temperature fluctuations about the mean are quoted by the manufacturer as being under 2 K. Temperature stabilization was performed with a precision of 1 K. The precision of temperature measurements in the interaction volume is estimated to be better than 2%.

2 Theoretical Background

The theory of stimulated Raman spectroscopy has been discussed in a great number of review articles (see for example [2]), so only the key aspects for temperature fit will be presented here. The SRS signal comes from the third-order nonlinear susceptibility $\chi^{(3)}$. Neglecting Doppler broadening and taking into account motional narrowing which occurs for overlapping lines in the isotropic Q-branch, an expression for $\chi^{(3)}$ can be derived as [1]

$$\chi^{(3)}_{(v,v+1)}(\omega) = \chi^{(3)}_{(\mathrm{NR})} - \frac{\mathrm{i}n_1}{\hbar}\sum_{JJ'}|\langle v|\bar{\alpha}|v+1\rangle|^2 \times \Delta\varrho^{(0)}_{(vJ)}G^{-1}_{J'J}(\omega)\,, \tag{1}$$

where the matrix G is defined as

$$G_{J'J}(\omega) = \mathrm{i}[\omega - \omega_{(v+1)J',vJ'} - n_B(\delta_{vJ'} + \mathrm{i}\gamma_{vJ'})] \times \delta(J'-J) + [1-\delta(J'-J)]n_B W_{J'J}\,. \tag{2}$$

In (1) and (2), n_1 is the density of optically active molecules, $\chi^{(3)}_{(\mathrm{NR})}$ is the nonresonant susceptibility, v is the vibrational quantum number of the lower state, $\bar{\alpha}$ is the isotropic part of the polarizability tensor, $\Delta\varrho^{(0)}_{(vJ)} = \varrho^{(0)}_{(vJ)} - \varrho^{(0)}_{(v+1)J}$ refers to the difference of number density of population between the initial and final states at equilibrium temperature, $\omega_{(v+1)J',vJ'}$ denotes the $Q(J')$ line position for an isolated molecule, n_B is the number density of perturbers, $\delta_{vJ'}$ is the density shift of the $Q(J')$ line, $\gamma_{vJ'}$ is the line broadening coefficient of the $Q(J')$ line, $W_{J'J}$ is the rotational energy transfer from J to J', and $\delta(J'-J)$ is the Kronecker delta function. $W_{J'J}, \gamma_{vJ'}, \delta_{vJ'}$ are assumed v-independent and the effect of the imaginary part of $W_{J'J}$ is considered as negligible. Let us note that for a mixture of n gases $W_{J'J}$ can be written as

$$W_{J'J} = \sum_{j=1}^{n} x_j W_{J'J}(1-j)\,, \tag{3}$$

where x_j is the mole fraction of gas j, and $W_{J'J}(1-j)$ denotes the relaxation matrix for the $(1-j)$ binary system. Similar equations apply to $\delta_{vJ'}$ and $\gamma_{vJ'}$. The rotational dependence of the collisional shift $\delta_{vJ'}$ being not clearly displayed experimentally, $\delta_{vJ'}$ is assumed to be J'-independent ($\delta_{vJ'} \cong \delta_v$). So δ_v can be factored out and applied as an overall frequency shift of the whole Q-branch. By explicitly taking into account the pure vibrational dephasing γ_v, the line broadening coefficients can be expressed as

$$\gamma_{vJ} = \gamma_J + \gamma_v\,, \tag{4}$$

where $\gamma_J = -\sum_{J'\neq J} W_{J'J}$ is the rotational inelastic broadening. $\Delta\varrho^{(0)}_{(vJ)}$ are calculated from the Boltzmann distribution.

In order to have an efficient method for fitting the temperature, (1) and (2) are transformed into matrix notation [19, 20, 29].

$$\sum_{JJ'}\Delta\varrho^{(0)}_{(vJ)}G^{-1}_{J'J}(\omega) = [\Delta\varrho^0]^t\mathbf{G}^{-1}[\mathbf{1}] \tag{5}$$

with $\mathbf{G} = \mathrm{i}\omega\mathbf{I} + \mathbf{K}$, where $[\mathbf{1}]$ is a column vector whose elements are all equal to one. We may then diagonalize $\mathbf{K}$ and define a new matrix

$$\mathbf{H} = \mathbf{A}^{-1}[\mathbf{1}]\,[\Delta\varrho^0]^t\mathbf{A}\,, \tag{6}$$

where $\mathbf{A}$ is the matrix of eigenvectors.

By defining h^v_J as the diagonal elements of $\mathbf{H}$ and λ^v_J as the eigenvalues of $\mathbf{K}$, (1) becomes

$$\chi^{(3)}_{(v,v+1)}(\omega) = \chi^{(3)}_{(\mathrm{NR})} - \frac{\mathrm{i}n_1}{\hbar}\sum_{JJ'}|\langle v|\bar{\alpha}|v+1\rangle|^2 \times \sum_J \frac{h^v_J}{\mathrm{i}\omega + \lambda^v_J}\,. \tag{7}$$

At high temperature, several vibrational levels are populated. By assuming that coupling between vibrational bands is negligible, the resultant $\chi^{(3)}(\omega)$ is just a sum over each

vibrational isolated band

$$\chi^{(3)}(\omega) = \sum_v \chi^{(3)}_{(v,v+1)}(\omega)\,. \tag{8}$$

By developing the complex values h_J^v and λ_J^v into real and imaginary parts,

$$h_J^v = p_J^v + \mathrm{i}q_J^v\,, \qquad \lambda_J^v = \Gamma_J^v - \mathrm{i}\omega_J^v\,, \tag{9}$$

and recalling that the SRS signal is proportional to $\mathrm{Im}\,\chi^{(3)}(\omega)$, we obtain

$$S(\omega) = \frac{n_1}{\hbar} \sum_v |\langle v|\bar{\alpha}|v+1\rangle|^2 \times \sum_J \frac{p_J^v \Gamma_J^v + q_J^v(\omega - \omega_J^v)}{(\Gamma_J^v)^2 + (\omega - \omega_J^v)^2}\,. \tag{10}$$

In the general formalism described above Doppler broadening has been neglected, which is not a realistic approximation when collisional narrowing appears at low density such as for the ν_1 band of CO_2 [20]. Let us also recall that Dicke narrowing leads to a reduction of the Doppler width resulting from velocity changing collisions. So, in a few particular cases, line mixing effects and Dicke narrowing should be simultaneously introduced in the lineshape calculation. The complex Galatry function [30] is an efficient soft-collision model which accounts for the effect of velocity-changing collisions and may be confidently used in many cases; its expression is

$$CG(x_J^v, y_J^v, z) = \frac{1}{\sqrt{\pi}} \int_0^\infty d\tau \exp\left[\mathrm{i}x_J^v\tau - y_J^v\tau + \frac{1}{2z^2}(1 - z\tau - e^{-z\tau})\right], \tag{11}$$

where the new characteristic parameters are

$$x_J^v = \frac{\omega - \omega_J^v}{\gamma_\mathrm{D}'}, \qquad y_J^v = \frac{\Gamma_J^v}{\gamma_\mathrm{D}'}, \qquad z = \frac{\beta}{\gamma_\mathrm{D}'}, \qquad \beta = \frac{kT}{2\pi m D}, \quad \text{and} \quad \gamma_\mathrm{D}' = \frac{\gamma_\mathrm{D}}{\sqrt{\mathrm{Log}\,2}}\,. \tag{12}$$

In (12), D is the optical diffusion coefficient and γ_D the Doppler width (HWHM). The variation of D as a function of pressure and temperature is expressed as

$$D = D_0\left(\frac{T}{T_0}\right)^m \frac{p_0}{p} \tag{13}$$

with usually $p_0 = 1$ atm and $T_0 = 273.15$ K. D_0 was taken from our previous studies [5, 17, 20] and m was fixed to 1.5, which is the value found in a study of Dicke narrowing in N_2 [31]. For the molecules considered here, Dicke narrowing appears at low pressure when the nonlinear pressure dependence of the density is negligible, so that the diffusion coefficient is simply inversely proportional to pressure.

The bandshape including Dicke and line mixing effects is then

$$S(\omega) = \frac{n_1}{\hbar} \sum_v |\langle v|\bar{\alpha}|v+1\rangle|^2 \sum_J [p_J^v\,\mathrm{Re}\{CG(x_J^v, y_J^v, z)\} + q_J^v\,\mathrm{Im}\{CG(x_J^v, y_J^v, z)\}]\,. \tag{14}$$

When the apparatus function is not negligible, a numerical convolution of $S(\omega)$ with a Gaussian function with half width γ_a is made ($\gamma_\mathrm{a} = 1.1 \times 10^{-3}\,\mathrm{cm}^{-1}$ HWHM). In fact, by fitting some strong isolated lines at low pressure (less than 10 Torr), we have found that the apparatus function is not exactly Gaussian, but is better represented by adding a Lorentzian part (less than $3 \times 10^{-4}\,\mathrm{cm}^{-1}$ HWHM). This Lorentzian part has a negligible influence in the present study. The SRS signal can be then calculated whatever the pressure and temperature, provided that the relaxation matrix W is completely determined. Due to the difficulties to measure and/or calculate all W elements, a few simple models are usually used such as the MEG and ECS-P laws [11]. For the MEG model, the upward rate of transitions from J to J' ($J' > J$) is described as [7]

$$W_{J'J}(1-j) = -\alpha\left(\frac{T}{T_\mathrm{ref}}\right)^{-N}\left(\frac{1 + aE_J/kT\delta}{1 + aE_J/kT}\right)^2 \times \exp(-\beta E_{J'J}/kT) \tag{15}$$

with α, N, δ, and β the temperature independent parameters, T_ref a reference temperature, $E_{J'J} = |E_{J'} - E_J|$ the energy gap, and a, a constant proportional to the duration of a collision. The ECS-P rate law allows the determination of all the relaxation matrix elements through the basis rate constants W_{0L} [9],

$$W_{J'J}(1-j) = (2J'+1)\exp[(E_{J'} + E_{J\rangle})/kT]\Omega_{J\rangle}^2 \times \sum_L \begin{pmatrix} J & J' & L \\ 0 & 0 & 0 \end{pmatrix}^2 \times (2L+1)\Omega_L^{-2} W_{0L}(1-j)\,, \tag{16}$$

where $J\rangle$ is the greater of J and J' and Ω the adiabatic factor calculated from the interaction length l_c. The basis rate constants are

$$W_{0L}(1-j) = -A_0(T/T_\mathrm{ref})^{-N}[L(L+1)]^{-\gamma}\,. \tag{17}$$

The rate-law parameters $(N, \alpha, \beta, \ldots)$ depend on the collisional binary system and are taken from our previous studies [8, 9, 11, 14, 17, 19].

The computer routine that we have developed allows us to fit the pressure and temperature and three other parameters which are an overall intensity scale factor A, a constant baseline offset B and an overall frequency shift Δ. The relative Raman intensity is then

$$I(\omega) = B + A\left[\int_{-\infty}^{+\infty} S(\omega_0 + \Delta) \times \exp -\frac{(\omega - \omega_0)^2}{(\gamma_\mathrm{a}/\sqrt{\log 2})^2}\,d\omega_0\right], \tag{18}$$

where S is a function of p and T.

Let us now examine in detail the dependence of the Raman intensity $I(\omega)$ versus pressure and temperature. In (1), $\Delta\varrho^{(0)}_{(vJ)}$ depends on temperature as the population of the states is given through the Boltzmann distribution. In (2), the density of perturbers has been expressed, using the second-

order virial coefficient B_v, by the usual simple expression

$$n_B = \frac{V_0}{2B_v}\left[-1+\left(1+\frac{4B_vP}{RT}\right)^{1/2}\right], \quad (19)$$

where P is the total pressure in the cell and V_0 the molar volume at STP. B_v is obtained with the virial coefficients B_{vij} of the $(i-j)$ binary systems [32–34]

$$B_v = \sum_{i=1}^{n}\sum_{j=1}^{n} B_{vij}x_ix_j\,, \quad (20)$$

with $B_{vij} = B_{vji}$ for any (i,j).

The temperature dependence of the B_{vij} coefficients has been empirically expressed by a polynomial series in powers of $1/T$:

$$B_{vij}(T) = \sum_{l=0}^{l_{max}} a_{ijl}T^{-l}\,, \quad (21)$$

where l_{max} is chosen in order to reproduce the experimental values of $B_{vij}(T)$ within the experimental uncertainties. The a_{ijl} coefficients are obtained by a least squares fit to experimental data [32–34]. $W_{J'J}$ and γ_J depend on temperature through the definitions given in (15)–(17). We have assumed that δ_v and γ_v are constant when expressed per unit of density (cm^{-1} amagat^{-1}). That is a correct approximation for N_2 and O_2, but not valid for CO_2, as shown later. When Doppler broadening is taken into account explicitly, the T dependence is expressed through (11)–(13). Let us also remark that the diffusion coefficient D is pressure dependent. If not directly available the virial coefficients and diffusion coefficients can be obtained from the Lennard-Jones parameters, in particular for the gas mixtures [32]. Due to the complexity of the problem the partial derivatives of P and T, which are necessary in the least squares fit, are calculated numerically.

3 Results and Discussion

Before discussing the results, let us give a few general aspects of the temperature fit. First of all, the highest pressure allowed by our procedure is determined by the limit of validity of (19) and from a more theoretical point of view by the limit of validity of the impact approximation. The parameters of the rate laws used are those given in [9, 11] for N_2–N_2, [14] for N_2–CO_2, [17] for O_2–O_2, and [19] for CO_2–CO_2. The spectroscopic parameters are those mentioned in the above references. For oxygen and nitrogen the vibrational broadening γ_v is negligible in the pressure range investigated in this study and δ_v has been fixed to the values measured at low densities. For all spectra used in this study, the precision of the fitted temperature ranges from 1.3 to 3.3% with a typical value of 2% for three times the standard deviation. This precision does not take into account the accuracy of the fitting parameters of the models.

Recent studies [11, 14] have shown that the calculated collapsed Q-branch would not match very well the experimental data when δ_v is fixed to the values obtained at low density, certainly due to imperfections in the calculation of the W matrix and/or to the influence of nonbinary collisions. As an example, a spectrum of pure nitrogen recorded at $P = 50$ bar and $T = 295$ K and calculated with the MEG law gives a fitted temperature of 365 K when δ_v is fixed to -3.5×10^{-3} cm^{-1} amagat^{-1} (low density value). In order to compensate for this particularity it is necessary to fit an overall frequency shift Δ. In that case we obtain $T_{fit} = 320$ K instead of 365 K, which is a significant improvement. So, we conclude that T and Δ should be simultaneously adjusted. We have also investigated whether pressure and temperature can be simultaneously determined. When the overlapping of $Q(J)$ lines is important so that no structure is visible, a strong correlation between Δ and p makes the fitting procedure unstable. Indeed, as shown in Fig. 1, a 25% variation of pressure leads to a modification of the spectral shape which looks like an overall frequency shift. So, in this work, we have been essentially interested in fitting the temperature.

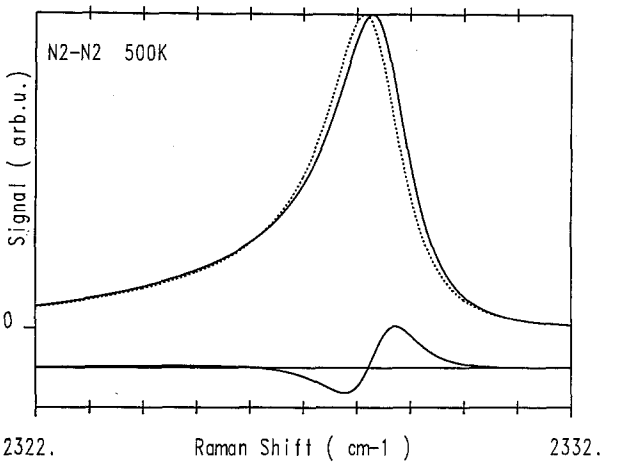

Fig. 1. Q-branch profiles calculated with the MEG model for pure nitrogen at $T = 500$ K, $P = 100$ bar (——) and $P = 125$ bar (· · · · · ·). The bottom trace shows the difference between the two spectra

The results for pure nitrogen are presented in Table 1. At 140 K and 0.98 bar both models give about the same

Table 1. Comparison between fitted temperature and thermocouple temperature for pure nitrogen with the MEG and ECS-P models and at various pressures. The numbers in square brackets indicate the deviation of the deduced temperatures from the reference temperature

$T_{thermocouple}$ [K]	p [bar]	T_{fit} [K]	
		MEG	ECS-P
140	0.98	132 [−8]	131 [−9]
295	18.0	323 [+28]	291 [−4]
	35.0	314 [+19]	268 [−27]
	50.0	320 [+25]	273 [−22]
	100.0	321 [+26]	274 [−21]
506	18.0	526 [+20]	482 [−24]
	35.0	524 [+18]	459 [−47]
	50.0	537 [+31]	460 [−46]
	75.0	551 [+45]	474 [−32]
	100.0	533 [+27]	445 [−61]
730	18.5	755 [+25]	691 [−39]
1260	1.0	1292 [+32]	1240 [−20]

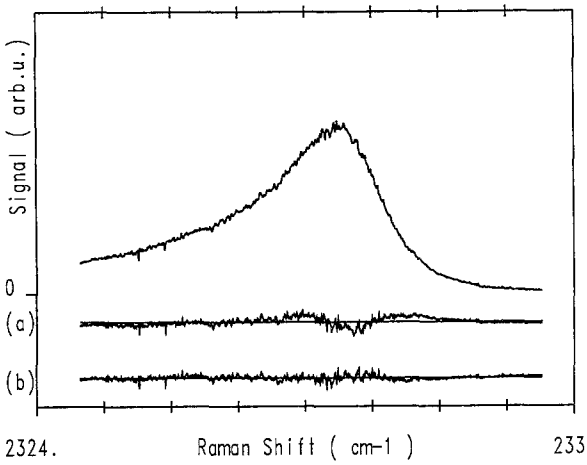

Fig. 2. Illustration of the ability of the MEG and ECS-P laws to provide a good spectral line shape by fitting the temperature. The upper trace gives the experimental SRS data of the isotropic Q-branch for N_2–N_2 at 506 K and 75 bar. The bottom traces display the residual given by the difference between the data and the calculation (a) with ECS-P and (b) with MEG

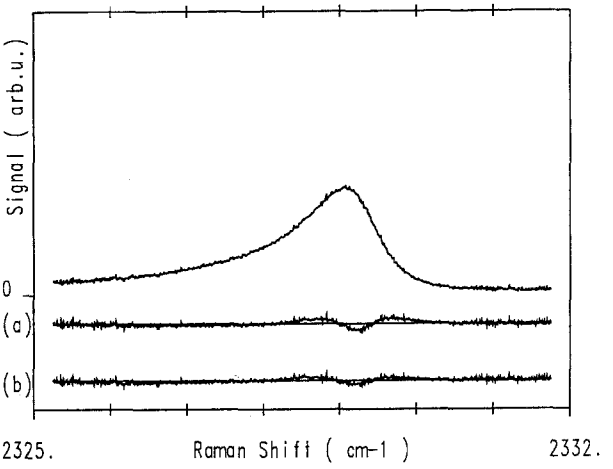

Fig. 3. Same as Fig. 2, but for N_2–CO_2 at 295 K and 14.3 bar

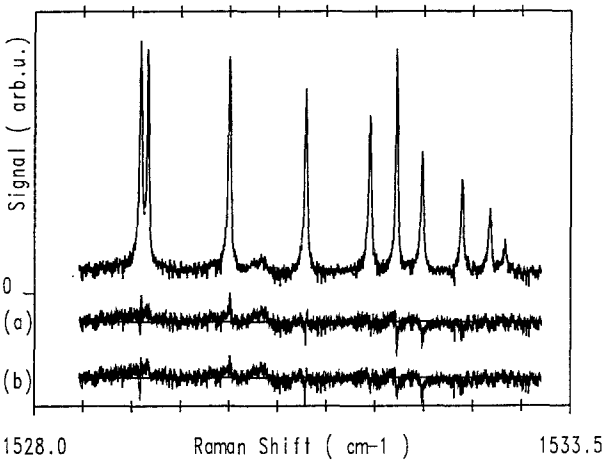

Fig. 4. Same as Fig. 2, but for O_2–O_2 at 1350 K and 0.98 bar. The spectrum ranges in the region of the first hot-band ($J = 1$ to 15) and includes two lines of the fundamental band ($J = 39$ and 41)

temperature. A too low temperature is found, which can be easily explained by the fact that the calculated line broadening coefficients at 140 K are smaller than the observed coefficients and by recalling that linewidths increase when temperature decreases. The discrepancies between the observed and calculated line broadening coefficients at 140 K (about 10%) are essentially due to the use of a very simple scale factor $[(T/T_{ref})^{-N}]$ for the calculation of the relaxation matrix elements. A more sophisticated law should be necessary to extrapolate the line broadening coefficients at low temperature (less than 295 K), and also at high temperature (greater than 1500 K). Even so the models can be used at low temperature and low pressure with relatively good confidence, a discrepancy of only 8–9 K being found. The results at 295 K and 506 K and medium pressure show that the MEG model systematically overestimates the temperature, whereas the ECS-P model underestimates it. The same phenomenon is found at 730 K and 18.5 bar. The results of the fit at 506 K and 75 bar are shown in Fig. 2 for the two models. The quality of the fit is better with the MEG model but the deviation of the fitted temperature from the reference temperature is larger with this model. As a consequence, the quality of the agreement between theory and experiment does not give necessary information on the quality of the agreement between the fitted temperature and the reference temperature. Large discrepancies between the two models are present, up to 88 K at 506 K and 100 bar. At 1260 K and 1 bar the fitted temperature is correct for both models what is not surprising because line mixing becomes negligible and the line-broadening coefficients are correctly reproduced at this temperature. In the case of the mixture N_2–CO_2 (Table 2) the results obtained at 295 K are similar to those found for pure nitrogen. Figures 3–4 indicate the quality of agreement between theory and experiment achieved for N_2–CO_2 at 295 K and 14.3 bar, and O_2–O_2 at 1350 K and 0.98 bar, respectively. Figure 4 shows that at low pressure the same agreement is obtained with the two models. Table 3 gives

Table 2. Same as Table 1, but for the mixture N_2–CO_2 (30% N_2, 70% CO_2)

$T_{thermocouple}$ [K]	p [bar]	T_{fit} [K]	
		MEG	ECS-P
295	5.3	315 [+20]	300 [+5]
	14.3	312 [+17]	281 [−14]
	23.4	321 [+26]	282 [−13]
	31.7	333 [+38]	293 [−2]

Table 3. Same as Table 1, but for pure oxygen

$T_{thermocouple}$ [K]	p [bar]	T_{fit} [K]	
		MEG	ECS-P
295	21.1	324 [+29]	304 [+9]
	50.7	288 [−7]	257 [−38]
446	6.4	450 [+4]	449 [+3]
	176.0	456 [−10]	413 [−33]
1350	0.98	1298 [−52]	1257 [−93]

a few examples for pure oxygen at three different temperatures. For this collisional system the differences between the models are a little smaller, the ECS-P always giving the lower temperatures.

For the CO_2–CO_2 system, we have made temperature fits on the spectra of the Fermi dyad $\nu_1/2\nu_2$. As shown in [19, 20], the collisional frequency shifts of the ν_1 and $2\nu_2$ Raman bands are different and temperature dependent. In fact, this temperature dependence does not perturb the temperature fit if an overall frequency shift Δ is adjusted. So, we fixed the collisional frequency shifts at their mean values in the temperature range 295–900 K [35]: -6.6×10^{-3}cm^{-1} amagat^{-1} and -9.5×10^{-3}cm^{-1} amagat^{-1} for ν_1 and $2\nu_2$, respectively. In contrast with the N_2 and O_2 systems discussed before, the vibrational contribution γ_v to the linewidth in CO_2 systems cannot be neglected [19, 20, 35], and its contribution is even preponderant at high pressures (typically above 0.5–1 bar for ν_1 band and above 10–30 bar for $2\nu_2$ band, at room temperature). The order of magnitude of γ_v in CO_2–CO_2 is about 4×10^{-3}cm^{-1} amagat^{-1}. The main goal of this work being a critical test of rate laws, the pressure was chosen in a range where collisional narrowing is crucial. The pressure ranges at each temperature are listed in Table 4 ($2\nu_2$ band) and Table 5 (ν_1 band). The data at 700 K and 900 K have been recently recorded [35], whereas those at 295 K and 500 K are from [19, 20]. At the pressures of recordings used to fit the temperature, the vibrational linewidth γ_v may have an important contribution to the band shape. The knowledge of this parameter and its T dependence are therefore essential. For both ν_1 and $2\nu_2$ bands, accurate values of γ_v have been obtained at 295, 500, 700, and 900 K [19, 20, 35]. The values are in the range $2.9–4.3 \times 10^{-3}$cm^{-1} amagat^{-1} (ν_1) and in the range $3.9–5.6 \times 10^{-3}$cm^{-1} amagat^{-1} ($2\nu_2$). The slight variation with temperature allowed us to consider only the mean values: 3.5 and 4.6×10^{-3}cm^{-1} amagat^{-1} for ν_1 and $2\nu_2$, respectively. This is also consistent with the fact that in the fitting procedure, γ_v expressed in density unit, is considered as constant. The results concerning the $2\nu_2$ band are gathered in Table 4 and an example of the quality of the fit is shown on Fig. 5 at 500 K and 1.09 bar. The agreement between theory and experiment is excellent with the ECS-P model. The temperature T_{fit} has been averaged over several spectra (3 or 4) recorded in the pressure domain indicated. The ECS-P model gives temperatures in very good agreement with those derived from the thermocouple readings. Similarly to the previous systems N_2–N_2, N_2–CO_2, and O_2–O_2, the MEG law leads to larger values of the temperature than the ECS-P does, which results in a great overestimation at high temperature. In the results given in Tables 1–4, the apparatus function has been neglected and in most cases, the Doppler effect has been disregarded. These broadening contributions to the lineshape have to be included in the fit of ν_1 band of CO_2, simultaneously with the collisional profile [20]. Indeed, this band undergoes at low pressure ($p \cong 0.01$–0.1 bar) both collisional narrowing due to rotational energy transfers and diffusional narrowing (Dicke narrowing) due to velocity changing collisions. The full bandwidth reaches a minimum of about 5×10^{-3} cm^{-1} at 0.3 bar, which is only

Table 4. Comparison between fitted temperature and thermocouple temperature for the $2\nu_2$ band of pure CO_2 with the MEG and ECS-P models. The fitted temperature is the averaged value over the pressure range indicated in the second column. The numbers in parenthesis represent the scatter of the averaged values

$T_{thermocouple}$ [K]	p [bar]	T_{fit} [K] average value	
		MEG	ECS-P
295	0.2–2.2	337(13) [+42]	309(7) [+14]
500	0.4–3.7	537(49) [+37]	493(29) [−7]
700	3.1–9.1	817(18) [+117]	707(19) [+7]
900	3.0–14.7	1036(61) [+136]	912(25) [+12]

Table 5. Same as Table 1, but for the ν_1 band of pure CO_2

$T_{thermocouple}$ [K]	p [bar]	T_{fit} [K]	
		MEG	ECS-P
295	0.00087	306 [+11]	306 [+11]
	0.0109	304 [+9]	303 [+8]
	0.0547	375 [+80]	323 [+28]

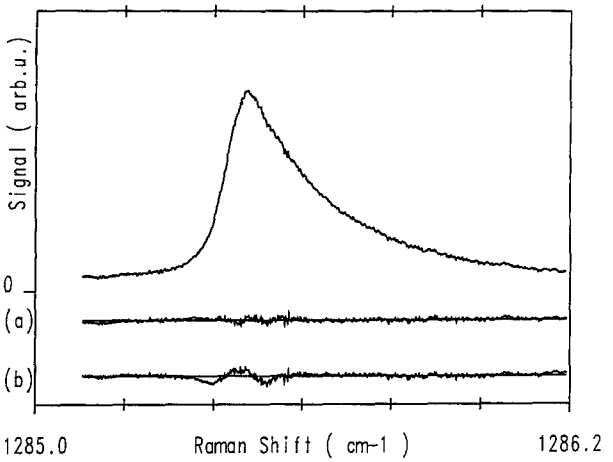

Fig. 5. Same as Fig. 2, but for the $2\nu_2$ band of CO_2–CO_2 at 500 K and 1.09 bar

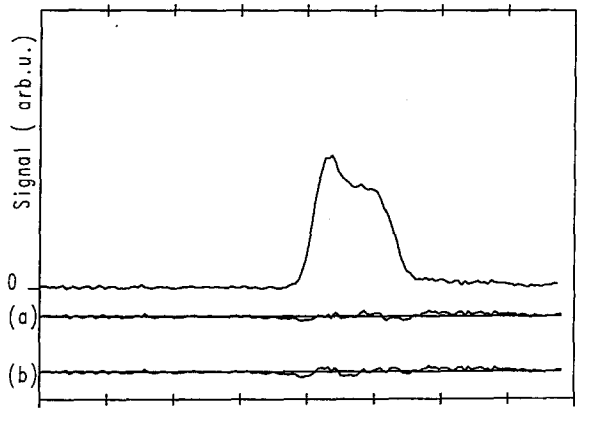

Fig. 6. Same as Fig. 2, but for the ν_1 band of CO_2–CO_2 at 295 K and 0.0109 bar

2.2 times the experimental resolution. Three spectra of the ν_1 band at room temperature have been fitted (Table 5). At very low pressure (0.00087 bar), no line mixing is present and thus no difference between the two models is observed. Increasing the pressure leads to the same conclusion, as above, for the comparison between MEG and ECS-P. Figure 6 gives a comparison between theoretical and observed spectra at 295 K and 0.0109 bar. No significant difference between the two models is observed. At pressure greater than 0.1 bar, the collisional linewidth γ_v plays an important role, whereas the influence of the relaxation model progressively disappears. So, above 0.1 bar, the temperature is mainly determined by the variation of γ_v, which has not been modeled here.

4 Conclusions

The fitting procedure developed here to measure temperature from experimental stimulated Raman spectra of simple molecules like N_2, O_2 and CO_2, takes into account the main sources of broadening in high-resolution spectroscopy: collisional broadening and line mixing, Doppler and Dicke effects, and the apparatus function. The routine has been written to extract the temperature also from CARS spectra, and thus is a general tool, for example, to compare relaxation models.

We evidenced the difficulty to simultaneously adjust pressure and temperature from unresolved band shapes. This difficulty is mainly due to the necessity to adjust an overall frequency shift to compensate for the lack of information on collisional frequency shift, and to a strong correlation between pressure and shift.

The test of two models (MEG and ECS-P), gave rise to the following conclusions. The temperatures determined from the MEG are higher than those determined from ECS-P for all systems (N_2, N_2–CO_2, O_2, CO_2). Very large temperature differences were obtained between the two models in a few cases such as for pure nitrogen at medium pressure. It seems clear that more sophisticated rotational relaxation models are needed to improve the temperature determination in a large pressure range. Spectra recorded at high pressure and high temperature should be also very useful to test and develop models. The influence of nonbinary collisions should be also considered for high-density spectra. No clear superiority of one model with respect to the other can be claimed for nitrogen and oxygen. In the case of pure CO_2 the fitted temperatures agree well with the thermocouple readings with the ECS-P model, whereas large discrepancies are observed with the MEG model.

A modelization of the temperature dependences of the vibrational linewidth γ_v of the Fermi dyad of CO_2 would provide the possibility of measuring the temperature at moderate pressures $p \geq 0.1$ bar from ν_1 spectra by including it in the routine.

Finally, Raman spectra recorded in a static cell by using a high-resolution scanning CARS spectrometer would be of interest for making a direct comparison with our SRS measurements.

Acknowledgements. This research was supported by the Conseil Régional de Bourgogne and the CNRS. We thank our colleagues from Dijon (SMIL) and Besançon (LPM) for their collaboration during these last years. We thank Pr. J. I. Steinfeld for reading of the manuscript. We would also to thank P. Michaux for his essential contribution in the technical part of the SRS spectrometer.

References

1. D.A. Greenhalgh: *Advances in Non-Linear Spectroscopy*, ed. by J.H. Clark, R.E. Hester (Wiley, New York 1988) p. 193
2. D. Robert: *Raman Spectroscopy Vibrational Spectra and Structure*, ed. by J.R. Durig (Elsevier, New York 1989) p. 17B
3. G. Millot, B. Lavorel, R. Saint-Loup, H. Berger: J. Phys. (Paris) **46**, 1925 (1985)
4. B. Lavorel, G. Millot, R. Saint-Loup, C. Wenger, H. Berger, J.P.Sala, J. Bonamy, D. Robert: J. Phys. (Paris) **47**, 417 (1986)
5. L.A. Rahn, R.E. Palmer: J. Opt. Soc. Am. B **3**, 1164 (1986)
6. J.P. Sala, J. Bonamy, D. Robert, B. Lavorel, G. Millot, H. Berger: Chem. Phys. **106**, 427 (1986)
7. M.L. Koszykowski, L.A. Rahn, R.E. Palmer, M.E. Coltrin: J. Phys. Chem. **91**, 41 (1987)
8. B. Lavorel, G. Millot, J. Bonamy, D. Robert: Chem. Phys. **115**, 69 (1987)
9. L. Bonamy, J. Bonamy, D. Robert, B. Lavorel, R. Saint-Loup, R. Chaux, J. Santos, H. Berger: J. Chem. Phys. **89**, 5568 (1990)
10. G.O. Sitz, R.L. Farrow: J. Chem. Phys. **93**, 7883 (1990)
11. J.I. Steinfeld, P. Ruttenberg, G. Millot, G. Fanjoux, B. Lavorel: J. Phys. Chem. **95**, 9638 (1991)
12. L. Bonamy, J.M. Thuet, J. Bonamy, D. Robert: J. Chem. Phys. **95**, 3361 (1991)
13. B. Lavorel, B. Oksengorn, D. Fabre, R. Saint-Loup, H. Berger: Mol. Phys. **75**, 397 (1992)
14. M.L. Gonze, R. Saint-Loup, J. Santos, B. Lavorel, R. Chaux, G. Millot, H. Berger, J. Bonamy, L. Bonamy, D. Robert: Chem. Phys. **148**, 417 (1990)
15. J. Bonamy, D. Robert, J.M. Hartmann, M.L. Gonze, R. Saint-Loup, H. Berger: J. Chem. Phys. **91**, 5916 (1989)
16. J. Bonamy, L. Bonamy, D. Robert, M.L. Gonze, G. Millot, B. Lavorel, H. Berger: J. Chem. Phys. **94**, 6584 (1991)
17. G. Millot, R. Saint-Loup, J. Santos, R. Chaux, H. Berger, J. Bonamy: J. Chem. Phys. **96**, 961 (1992)
18. G. Millot, C. Roche, R. Saint-Loup, R. Chaux, H. Berger, J. Santos: Chem. Phys. (in press)
19. B. Lavorel, G. Millot, R. Saint-Loup, H. Berger, L. Bonamy, J. Bonamy, D. Robert: J. Chem. Phys. **93**, 2176 (1990)
20. B. Lavorel, G. Millot, R. Saint-Loup, H. Berger, L. Bonamy, J. Bonamy, D. Robert: J. Chem. Phys. **93**, 2185 (1990)
21. G.J. Rosasco, L.A. Rahn, W.S. Hurst, R.E. Palmer, S.M. Dohne: J. Chem. Phys. **90**, 4059 (1989)
22. J.P. Looney, G.J. Rosasco, L.A. Rahn, W.S. Hurst, J.W. Hahn: Chem. Phys. Lett. **161**, 232 (1989)
23. R. Chaux, C. Milan, G. Millot, B. Lavorel, R. Saint-Loup, J. Moret-Bailly: J. Opt. (Paris) **19**, 3 (1988)
24. B. Lange, J. Wolfrum: Appl. Phys. B **51**, 53 (1990)
25. S. Kröll, P.E. Bengtsson, M. Alden, D. Nilsson: Appl. Phys. B **51**, 25 (1990)
26. F.M. Porter, D.A. Greenhalgh, P.J. Stopford, D.R. Williams, C.A. Baker: Appl. Phys. B **51**, 31 (1991)
27. M. Woyde, W. Stricker: Appl. Phys. B **50**, 519 (1990)
28. E. Diessel, T. Dreier, B. Lange, J. Wolfrum: Appl. Phys. B **50**, 39 (1990)
29. M.L. Koszykowski, R.L. Farrow, R.E. Palmer: Opt. Lett. **10**, 478 (1985)
30. L. Galatry: Phys. Rev. **122**, 1218 (1961)
31. G. Millot: Dissertation, Dijon (1986)
32. J.O. Hirshfelder, C.F. Curtis, R.B. Bird: *Molecular Theory of Gases and Liquids* (Wiley, New York 1954)
33. J.M. Dymond, E.B. Smith: *The Virial Coefficients of Pure Gases and Mixtures*, A Critical Compilation (Clarendon, Oxford 1980)
34. D.E. Gray: *American Institute of Physics Handbook*, 3rd edn. (McGraw-Hill, New York 1972)
35. B. Lavorel: Unpublished results